

# Physical Origin of the Quadrupole Out-of-Plane Magnetic Field in Hall-MHD Reconnection

Dmitri A. Uzdensky\* and Russell M. Kulsrud†

*Princeton University Observatory and Princeton Plasma Physics Laboratory*

*– Center for Magnetic Self-Organization (CMSO), Princeton, NJ 08544*

(Dated: May 11, 2006)

## Abstract

A quadrupole pattern of the out-of-plane component of the magnetic field inside a reconnection region is seen as an important signature of the Hall-magnetohydrodynamic (Hall-MHD) regime of reconnection. It has been first observed in numerical simulations and just recently confirmed in the MRX (Magnetic Reconnection Experiment) [M. Yamada, H. Ji, S. Hsu, T. Carter, R. Kulsrud, N. Bertz, F. Jobes, Y. Ono, and F. Perkins, *Phys. Plasmas* 4, 1936 (1997)] and also seen in spacecraft observations of Earth's magnetosphere. In this study, the physical origin of the quadrupole field is analyzed and traced to a current of electrons that flows along the lines in and out of the inner reconnection region to maintain charge neutrality. The role of the quadrupole magnetic field in the overall dynamics of the reconnection process is discussed. In addition, the bipolar poloidal electric field is estimated and its effect on ion motions is emphasized.

PACS numbers: 52.30.Cv, 52.30.Ex, 52.35.Vd, 94.05.-a, 94.30.cp, 96.60.Iv

---

\*Electronic address: uzdensky@astro.princeton.edu

†Electronic address: rmk@pppl.gov

## I. INTRODUCTION

Ever since it was established that the classical Sweet–Parker reconnection model [2, 3, 4] with Spitzer resistivity is too slow and that the Petschek [5] fast-reconnection mechanism cannot be realized in resistive MHD with uniform resistivity [6, 7, 8, 9, 10]), theoretical studies of fast reconnection have proceeded as a competition between two schools of thought. The first one invokes the idea of enabling the Petschek mechanism by a strongly localized anomalous resistivity due to plasma micro-instabilities triggered when a certain current threshold is exceeded [9, 10, 11, 12]. The second, commonly referred to as the Hall reconnection mechanism, relies on the two-fluid effects that become important when the reconnection layer becomes so thin that ion and electron motions decouple from each other [13, 14, 15, 16, 17]. In reality, as the layer gets thinner, the Hall term becomes more and more important, but it is possible that the condition for anomalous resistivity is reached first. If this happens, then the enhanced collision rate due to fluctuations allows electrons to flow across the field lines instead of having to flow rapidly along them to preserve charge neutrality (see below). This will weaken or remove the Hall effect on reconnection. On the other hand, it may be that a stable two-fluid flow pattern is established first, before the instabilities that lead to anomalous resistivity are triggered. Then reconnection would proceed by the Hall mechanism.

In the present study we focus on the Hall-magnetohydrodynamic (Hall-MHD) regime of reconnection. More specifically, our main objective is to understand the physical origin of the quadrupole pattern of the out-of-plane magnetic field that arises inside the reconnection region in this regime. We shall call it “the quadrupole field” for short. The quadrupole field is widely accepted as one of the most important signatures of the two-fluid effects

in the reconnection process. The reason for this is the following. Consider the simplest two-dimensional (2D) reconnection configuration (displayed in Fig. 1a), with  $z$  marking the ignorable direction, and  $x$  and  $y$  forming the so-called reconnection plane. Let us assume that there is no guide field, that is, assume that the magnetic field lines above and below the reconnection layer lie exactly in the reconnection plane (“null-helicity” reconnection). Then, in simple resistive magnetohydrodynamics (MHD) there is no mechanism that would produce an out-of-plane ( $z$ ) component of the magnetic field anywhere in the reconnection region; this is basically a consequence of the symmetries inherent to the resistive MHD equations. However, when electron and ion flows decouple from each other, that is when two-fluid effects become important, those symmetries are no longer present, since charge carriers of different sign now move differently. As a result, an out-of-plane component of the magnetic field may develop somewhere inside the layer. Thus, the emergence of this field is a tell-tale sign of the transition from resistive to two-fluid (e.g., Hall) regime of reconnection. For example, imagine a situation where one studies a reconnection process in a lab with limited diagnostic capabilities, say, with only magnetic probes but with no ability to measure plasma densities, temperatures, velocities, etc. Then one is not able to determine the ion skin depth and ion Larmor radius to compare them with the measured reconnection layer thickness. However, a mere detection of the  $z$ -component of the magnetic field in the layer will immediately and unambiguously reveal that one deals with a two-fluid reconnection regime.

The presence of an out-of-plane magnetic field with a quadrupole structure in the context of the Hall-MHD regime of collisionless reconnection was first suggested by Sonnerup [13] (see also the work of Terasawa [18] in the context of tearing instability in the Earth magnetotail). Since then, the quadrupole field has been observed in many numerical simulations of collisionless reconnection [14, 15, 16, 17, 19, 20, 21, 22]. It has also been detected in space

in-situ measurements by the *Polar* and *Cluster* spacecraft flying through the Earth magnetotail and the magnetopause [23, 24, 25]. The quadrupole magnetic field pattern has long evaded direct experimental detection in laboratory plasma experiments but just recently has finally been confirmed [26] in the Magnetic Reconnection Experiment (MRX) [1]. A similar result has recently been reported in the Swarthmore Spheromak Experiment (SSX) in a somewhat different type of a neutral sheet [27]. These experimental detections raise the need for a better theoretical understanding of the generation mechanism for the quadrupole field, which in our view is still lacking despite the great wealth of numerical data.

Our paper is structured as follows. In Sec. II we propose a basic physical explanation of how an out-of-plane magnetic field is generated in an electron MHD (eMHD) reconnection layer and why it inevitably has a quadrupole pattern. We start this section by discussing our physical assumptions (Sec. II A); then we present a simple physical description of the mechanism by which the quadrupole field is produced (Sec. II B); and, finally, we illustrate our ideas by an analytical calculation of the toroidal (e.g., out-of-plane) field in the X-point configuration (Sec. II C). In Sec. III we step back from our specific example of Sec. II C and derive some general results pertinent to stationary incompressible ideal eMHD in 2.5 dimensions. Thus, in Sec. III A we establish proportionality between three important quantities: the volume per poloidal flux computed along a field line, the poloidal (e.g., in-plane) electron stream function, and the electron contribution to the toroidal magnetic field. In particular, we show that, as long as ion currents are neglected in Ampere’s law and the electrons are magnetized, the toroidal magnetic field is constant along electron streamlines; correspondingly, the toroidal electron velocity has to be constant along poloidal magnetic field lines. This means at least that inside the reconnection layer, at scales smaller than the ion inertial scale (but outside the inner electron dissipation region), one cannot invoke

the usual explanation for the quadrupole field as being created by differential stretching of the poloidal field lines due to a non-uniform toroidal electron flow. It then follows that the toroidal field has to be generated in the transition region in the outskirts of the reconnection layer, where the ion-current contribution is still important. To study this process, we consider the three-dimensional shape of the field lines and show that the toroidal separation  $\Delta z$  between a given fluid element on a line and the tip of the line at the  $x = 0$  plane is related to the volume per flux integral (Sec. III B). This enables us to calculate the toroidal electron velocity (Sec. III D) and hence estimate when (i.e., how close to the separatrix) electron inertia becomes important in the generalized Ohm law (Sec. III E). Finally, we argue that the toroidal velocity of the field lines should be attributed to an  $\mathbf{E} \times \mathbf{B}$  drift of electrons; this requires the presence of a bipolar poloidal electric field which we compute in Sec. III F. This electric field is also an important signature of the two-fluid effects in reconnection; in particular, it is responsible for accelerating ions into the reconnection layer, resulting in an effective ion heating. We summarize our work in Sec. IV.

## II. HOW IS THE QUADRUPOLE FIELD GENERATED IN THE RECONNECTION REGION?

### A. Physical Assumptions

First, let us discuss the physical assumptions that we adopt in this paper. These assumptions are aimed at making the problem tractable while still realistic and complex enough to provide a useful physical picture of a reconnecting current layer in the Hall-MHD regime. While doing this, we pay special attention to the conditions relevant to the MRX experiment.

We will be mostly interested in the inner structure of the reconnection layer at scales (in

the direction across the layer) smaller than the ion collisionless skin depth defined as

$$d_i \equiv \frac{c}{\omega_{pi}} = c \sqrt{\frac{m_i}{4\pi n_e e}}. \quad (1)$$

Provided that there is some ion heating available, and in the absence of a strong guiding field, the ion gyro-radius,  $\rho_i$ , is comparable to  $d_i$  in this region, and so ions can be regarded as unmagnetized. Thus, their motion is not strongly affected by the small-scale magnetic structures that characterize the inner part of the reconnection layer considered in this paper. On these small scales, the motion of ions is slow and smooth; the ion density then cannot develop structure on these scales. We shall therefore treat ions as providing a neutralizing background, which, for simplicity, we shall take to be uniform. Also, for the most part, we shall assume them to be motionless, that is we shall neglect the ion contribution to the electric current. However, as we will show, the poloidal ion current in the outer region of the layer actually plays an important role in the generation of the quadrupole field.

In contrast to ions, electrons have very small gyro-radii and are well magnetized everywhere except in a small vicinity of the X-point. Thus, it is appropriate to use the framework of Hall MHD (or electron MHD) in most of the region under consideration. This framework is characterized as a two-fluid approach where the magnetic field is frozen into electrons but not into ions. An equivalent formulation is to use a generalized Ohm law (i.e., electron equation of motion) that includes the Hall term. On the other hand, since we are interested in scales that are much larger than the size of the inner electron diffusion region, we shall, in our analysis of the generalized Ohm law, neglect both the electron inertia term (although we shall estimate its contribution in Sec. III E) and the resistive term that arises due to normal particle-particle collisions (i.e., classical Spitzer resistivity) or due to wave-particle collisions (anomalous resistivity). At the same time, we shall include the electron pressure gradient

term, assuming, however, that the electron pressure tensor is isotropic. This assumption is justified if the system is not entirely collisionless. That is, we assume that collisions are rare enough for collisional resistivity to be negligible, but, at the same time, frequent enough to restore the electron pressure isotropy throughout most of the reconnection region. This is in fact consistent with the conditions encountered in the MRX experiment, where collisions are always present at some level [26].

Next, due to the charge neutrality condition (valid provided that the scales under consideration are still much larger than the Debye length), the electron density has to be equal to that of the ions. Since we assume that latter to be uniform, we require the electron density to be also uniform and hence the electron flow to be incompressible.

Finally, we assume that the reconnection layer is in a quasi-steady state, that it has a translational symmetry in one ( $z$ ) direction, and that there is no guide magnetic field (that is no externally imposed toroidal magnetic field).

Thus, from the above considerations, the set of physical assumptions can be summarized as *ideal incompressible 2.5-D steady-state electron MHD* without a guide field [28].

## **B. A Simple Physical Picture of the Quadrupole Field Generation**

We first describe the basic physical picture of how the quadrupole out-of-plane magnetic field naturally arises in electron MHD. Consider an incoming flux tube as it moves deeper and deeper into the (ion-scale) reconnection region toward the X-point (Fig. 1a). The poloidal magnetic field in the central part of the tube near  $x = 0$  has to decrease, and hence the volume of this central part has to expand. Since electrons are tightly coupled to magnetic field lines, this expansion would lead to a drop in electron density. However, the ions are

not magnetized and their density does not decrease. Therefore, since almost perfect charge neutrality is to be maintained, a very small poloidal electric field arises and it immediately pulls the electrons along the field lines inward from the outer parts of the flux tube into this central region. Owing to the very large mobility of electrons along the field (inversely proportional to  $m_e$ ), this parallel electric field is negligibly small.

As a result, we get a strong inflow of electrons along the poloidal magnetic field in the upstream region (Fig. 1b). This inflow rapidly accelerates as the field line approaches the separatrix, because of the rapidly increasing rate of flux-tube expansion near the X-point. In the downstream region, the direction of the electron flow reverses: as a newly reconnected field line moves away from the X-point, the volume of its central part decreases and so the electrons are squeezed out and flow rapidly outward along the field (Fig. 1c). As the field line moves further away, this outflow gradually decelerates. The resulting overall picture of the electron flow is shown in Fig. 1c; once again, the main feature is the rapid inflow of electrons just above the separatrix followed by a rapid outflow just below the separatrix.

This pattern of electron motion plays an important role in eMHD reconnection, since there is a poloidal electric current associated with the flow of electrons. By Ampere's law, this current generates a quadrupole toroidal magnetic field concentrated along the separatrix (see Fig. 1d). This is our picture for the origin of the quadrupole field.

The orientation of this field is always such that the toroidal field in the upper right and lower left quadrants is directed away from the viewer, whereas the toroidal field in the lower right and the upper left quadrants is directed towards the viewer. It is interesting to note that this orientation is universal, i.e., independent of the direction of the poloidal field.



### C. An Analytical Example: a Simple X-point Configuration

To illustrate this mechanism, we present a very simple calculation of the toroidal field based on the simplest possible poloidal field configuration relevant to the reconnection problem. This configuration is of course the X-point configuration that we now describe.

Consider the central part of a reconnecting current layer. Let  $L$  be the half-width and  $\delta \ll L$  be the half-thickness of the layer. Let us choose a Cartesian coordinate system  $(x, y, z)$  with  $x$  being the direction along the layer,  $y$  across the layer, and  $z$  in the ignorable direction. We shall refer to the plane of reconnecting field (i.e., the  $xy$  plane) as the poloidal plane and the  $z$  direction as the toroidal direction. We set the origin  $x = 0 = y$  exactly at the X-point and assume mirror symmetry with respect to the  $xz$  and  $yz$  planes as well as the translational symmetry in the  $z$  direction (see Fig. 2). We also assume steady state.

We are interested in a small vicinity of the X-point, which means that we consider locations with  $x \ll L$  and  $y \ll \delta$ . In this region the poloidal magnetic field can be generically represented by a simple X-point configuration. In terms of the poloidal flux function  $\Psi(x, y, t)$  this can be written in the appropriate gauge as

$$\Psi(x, y, t) = -cE_z t + \frac{B_0 \delta}{2} \left( \frac{y^2}{\delta^2} - \frac{x^2}{L^2} \right), \quad (2)$$

with  $B_{\text{pol}} = \nabla \Psi \times \hat{z}$ .

This expression serves as the definition of the scales  $L$  and  $\delta$ . The first term in this expression is just the instantaneous value of the flux at the origin (which we can define as the flux that has reconnected since  $t = 0$ ). As reconnection proceeds, it increases at a constant rate equal to  $-cE_z = |cE_z| > 0$ , where  $E_z < 0$  is the toroidal electric field (which is uniform in steady state reconnection). The quantity  $B_0$  represents the reconnecting magnetic field just outside the layer:  $B_x(x = 0, y = \delta) = B_0$ . The poloidal magnetic field components

corresponding to this flux function are:

$$B_x = \partial_y \Psi = B_0 \frac{y}{\delta}, \quad (3)$$

$$B_y = -\partial_x \Psi = B_0 \frac{\delta}{L} \frac{x}{L}. \quad (4)$$

For convenience, we introduce dimensionless variables by rescaling  $x$ ,  $y$ ,  $\mathbf{B}$ ,  $\Psi$ , and  $E_z$  as

$$\begin{aligned} \bar{x} &\equiv \frac{x}{L}, & \bar{y} &\equiv \frac{y}{\delta} \\ \bar{\mathbf{B}} &\equiv \frac{\mathbf{B}}{B_0}, & \bar{\Psi} &\equiv \frac{\Psi}{B_0 \delta}, & \bar{E} &\equiv \frac{cE_z}{B_0 \delta}. \end{aligned} \quad (5)$$

Then equation (2) can be written as

$$\bar{\Psi}' \equiv \bar{\Psi} + \bar{E}t = \bar{\Psi}(x, y) - \bar{\Psi}(0, 0) = \frac{\bar{y}^2}{2} - \frac{\bar{x}^2}{2}. \quad (6)$$

Correspondingly, the shape of a given field line  $\bar{\Psi}$  is given (in the two upper quadrants)

by

$$\bar{y}(\bar{x}, \bar{\Psi}) = \sqrt{2\bar{\Psi}' + \bar{x}^2}. \quad (7)$$

Now we want to calculate the motion of the electron fluid. It is completely determined by two conditions: flux-freezing in the poloidal plane (which is not spoiled by the pressure gradient term in the generalized Ohm law, as we shall discuss later) and incompressibility. In order to get an explicit expression for the electron velocity, let us consider the trajectory  $\bar{X}(t)$ ,  $\bar{Y}(t)$  of an electron fluid element. As it moves through the layer, the given fluid element always stays on a field line with constant  $\bar{\Psi}$ ; thus, as one follows its motion,  $\bar{\Psi}' = \bar{\Psi} + \bar{E}t$  varies with time. Correspondingly, the trajectory of the element has to satisfy

$$\bar{Y}(t) = \sqrt{2(\bar{\Psi} + \bar{E}t) + \bar{X}^2(t)}. \quad (8)$$

Next, the incompressibility condition implies that the volume per unit flux following an electron fluid element,  $V(\bar{X}, \bar{\Psi}') = V[\bar{X}(t), \bar{\Psi} + \bar{E}t]$ , has to be conserved. Here,  $V(\bar{X}, \bar{\Psi}')$  is

measured along the line  $\bar{\Psi}'$  from the  $y$ -axis ( $\bar{x} = 0$ ) in the case of a field line in the upstream region (and from the  $x$ -axis,  $\bar{y} = 0$ , in the case of a field line in the downstream region), up to the fluid element under consideration. For example, in the upstream region we thus have

$$V[X(t), \Psi'] \equiv \int_0^{l(X)} \frac{dl}{|B_{\text{pol}}|} \Big|_{\Psi=\text{const}} = \int_0^{X(t)} \frac{dx}{|B_x|} \Big|_{\Psi=\text{const}} = \text{const}. \quad (9)$$

Using the expression (3) for  $B_x$  and (7) for the field line shape  $\bar{y}(\bar{x}, \bar{\Psi})$ , we get

$$V[\bar{X}(t), \bar{\Psi}'] = \frac{L}{B_0} \int_0^{\bar{X}(t)} \frac{d\bar{x}}{|\bar{y}(\bar{x}, \bar{\Psi})|} \Big|_{\Psi=\text{const}} = \frac{L}{B_0} \log \left| \frac{\bar{X}(t) + \sqrt{\bar{X}^2(t) + 2\bar{\Psi}'(t)}}{\sqrt{2\bar{\Psi}'(t)}} \right| = \text{const}. \quad (10)$$

Hence, the trajectory is given by  $(\bar{X}(t) + \sqrt{\bar{X}^2(t) + 2\bar{\Psi}'})/\sqrt{2\bar{\Psi}'} = \text{const}$ , that is  $\bar{X}(t)/\sqrt{2\bar{\Psi}'(t)} = \text{const}$ . Using (8), we also get a similar expression for  $\bar{Y}(t)$ . Thus,

$$\bar{X}(\bar{X}_0, t) = \xi(\bar{X}_0, \bar{\Psi}) \sqrt{2|\bar{\Psi} + \bar{E}t|}, \quad (11)$$

$$\bar{Y}(\bar{X}_0, t) = \eta(\bar{X}_0, \bar{\Psi}) \sqrt{2|\bar{\Psi} + \bar{E}t|}, \quad (12)$$

where  $\eta = \sqrt{\xi^2 \pm 1}$ , and where we take “+” in the upstream region and “-” in the downstream region. The constant parameters  $\xi$  and  $\eta$  represent the initial position of the electron fluid element at  $t = 0$ .

Differentiating these expressions with respect to time and using  $d\bar{\Psi}'/dt = \bar{E}$ , we obtain the electron velocity field at any point  $(\bar{x}, \bar{y})$ :

$$\bar{v}_{\bar{x}}^{(e)}(\bar{x}, \bar{y}) = \frac{\bar{x}}{2} \frac{\bar{E}}{\bar{\Psi}'(\bar{x}, \bar{y})} = -\bar{x} \frac{|\bar{E}|}{\bar{y}^2 - \bar{x}^2}, \quad (13)$$

$$\bar{v}_{\bar{y}}^{(e)}(\bar{x}, \bar{y}) = \frac{\bar{y}}{2} \frac{\bar{E}}{\bar{\Psi}'(\bar{x}, \bar{y})} = -\bar{y} \frac{|\bar{E}|}{\bar{y}^2 - \bar{x}^2}. \quad (14)$$

Notice that  $\bar{v}_{\bar{y}}^{(e)}/\bar{v}_{\bar{x}}^{(e)} = \bar{y}/\bar{x}$ , so electrons flow along purely radial lines, inward in the upstream region and then outward in the downstream region. Even though all the streamlines converge to the X-point in the upstream region (and fan out of the X-point in the downstream

region) the motion is incompressible since the magnitude of the velocity diverges near the origin. Also note that if the above velocity field holds, electrons never actually cross the separatrix; they all go through the X-point. This is of course an artifact of our ideal eMHD assumption.

This poloidal electron velocity field results in a poloidal electric current:

$$j_x^{(e)} = -en_e v_x^e = -en_e L \bar{v}_x^e, \quad (15)$$

$$j_y^{(e)} = -en_e v_y^e = -en_e \delta \bar{v}_y^e. \quad (16)$$

This current in turn produces a toroidal magnetic field. According to Ampere's law we have

$$\partial_y B_z^{(e)} = \frac{4\pi}{c} j_x^{(e)} = \frac{4\pi n_e e}{c} L |\bar{E}| \frac{\bar{x}}{2\bar{\Psi}'(\bar{x}, \bar{y})}, \quad (17)$$

$$\partial_x B_z^{(e)} = -\frac{4\pi}{c} j_y^{(e)} = -\frac{4\pi n_e e}{c} \delta |\bar{E}| \frac{\bar{y}}{2\bar{\Psi}'(\bar{x}, \bar{y})}. \quad (18)$$

We can thus compute the resulting toroidal field by integrating either of these equations while taking into account that  $B_z(0, y) = 0 = B_z(x, 0)$  because of symmetry. In the upstream region it is convenient to integrate  $\partial_x B_z^{(e)}(x, y)$  with respect to  $x$  at constant  $y$  starting with  $x = 0$ . (In the downstream region, it is convenient to do the opposite.) Thus we can write:

$$B_z(\bar{x}, \bar{y} > \bar{x}) = \int_0^{\bar{x}} L \partial_x B_z d\bar{x} = -\frac{4\pi n_e e}{c} \delta L |\bar{E}| \bar{y} \int_0^{\bar{x}} \frac{d\bar{x}}{2\bar{\Psi}'(\bar{x}, \bar{y})}. \quad (19)$$

Using the expression (6) for  $\bar{\Psi}'(\bar{x}, \bar{y})$ , we get

$$B_z(\bar{x}, \bar{y}) = -\frac{1}{2} B_0 Q \log \left| \frac{\bar{y} + \bar{x}}{\bar{y} - \bar{x}} \right|, \quad (20)$$

where we define a dimensionless constant

$$Q \equiv \frac{4\pi n_e e}{c B_0} \delta L |\bar{E}| = \frac{\delta}{d_i} \frac{L}{V_A} |\bar{E}|. \quad (21)$$

Expression (20) is actually valid in both the upstream and downstream regions. We note that a very similar expression was obtained, in the eMHD framework, in Ref. [15].

We can rewrite the coefficient  $Q$  in a different form by expressing the reconnection electric field  $\bar{E}$  in terms of the other parameters of the reconnection region. Indeed, let  $v_{\text{rec}}$  be the reconnection velocity,  $v_{\text{rec}} = -v_y(x = 0, y \gg \delta)$ . Then  $|E_z| = v_{\text{rec}}B_0/c$  and hence  $|\bar{E}| = v_{\text{rec}}/\delta$ . Then, we get

$$Q = \frac{L}{d_i} \frac{v_{\text{rec}}}{V_A} = C \frac{\delta}{d_i} \frac{u}{V_A}, \quad (22)$$

where  $u$  is the velocity of the flow out of the layer, and where we define a new dimensionless parameter  $C$ :

$$C \equiv \frac{Lv_{\text{rec}}}{\delta u} = O(1). \quad (23)$$

Because of the condition of overall mass conservation we expect  $C$  to be of order unity.

Usually, one expects the thickness  $\delta$  of a Hall-MHD reconnection region to be comparable to the ion collisionless skin depth  $d_i$  and the outflow velocity  $u$  to be of order  $V_A$ . Thus, equation (22) tells us that the proportionality coefficient  $Q$  is, generally speaking, expected to be of order unity. In practice, however,  $Q$  may significantly deviate from unity for any specific physical system. For example, in the MRX experiment one often encounters  $\delta \simeq d_i/3$  and  $u < V_A$ , so  $Q$  can be smaller than  $1/3$ .

The reader should be warned that formula (20) only applies to our specific example for the poloidal field, eq. (2), and may not be applicable to various configurations realized in some numerical simulations and in the MRX. We chose this specific example because of its simplicity and clarity and we leave more complicated poloidal field structures for a future study. We believe that the most physically-relevant among these other structures is a configuration with an inner electron current sheet (electron dissipation region) of a finite width in the  $x$ -direction.

As we see from equation (20), in the simple X-point configuration considered in this

section, the assumptions of ideal eMHD lead to a logarithmic divergence of  $B_z$  at the separatrix  $\bar{y} = \bar{x}$ . Later, in Sec. III E we shall discuss how this singularity is removed by including finite electron inertia. We also see that  $B_z$  in our solution is constant along straight radial rays  $y = \text{const} \cdot x$ . In reality we expect electron inertia and other non-ideal effects to intervene and break this idealized picture near the separatrix. However, we believe that the main tendency for the constant- $B_z$  contours to be strongly elongated along the separatrix will survive. In fact, this overall behavior is in a very good agreement with the results of numerical simulations [15, 16, 19, 20, 21, 22], and is also consistent with the experimental data [26].

### III. STATIONARY IDEAL INCOMPRESSIBLE EMHD IN 2.5 DIMENSIONS: GENERAL RESULTS

In this section we step back from the particular example of the previous section and derive several general results that are valid in steady-state 2D incompressible eMHD for an arbitrary poloidal field structure.

#### A. General relationships between toroidal magnetic field, electron stream function and the volume per flux in eMHD

First we introduce three important functions: the volume-per-flux integral  $V(x, \Psi)$ , the electron stream function  $\Phi_e$  and the (electron contribution to) the toroidal magnetic field  $B_z$ . We derive important relationships between these functions and discuss their implications.

The volume-per-flux integral  $V(x, \Psi)$  is defined (in the upstream region), as in the last

section, by

$$V(x, \Psi) \equiv \int_0^x \frac{dl}{|B|} \Big|_{\Psi} = \int_0^x \frac{dl_{\text{pol}}}{|B_{\text{pol}}|} \Big|_{\Psi}. \quad (24)$$

where, in the last expression, the integration is performed along a given poloidal line,  $\Psi$ , from the  $y$ -axis  $x = 0$  to the given point  $(x, \Psi)$ . A similar expression can be defined in the downstream region.

The electron stream function  $\Phi_e(x, y)$  is defined, for an incompressible flow,  $\nabla \cdot \mathbf{v}^{(e)} = 0$ , by the poloidal electron velocity as

$$\mathbf{v}_{\text{pol}}^{(e)} = [\nabla \times (\Phi_e \hat{z})] = [\nabla \Phi_e \times \hat{z}]. \quad (25)$$

For definiteness, we choose the streamline corresponding to zero  $\Phi_e$  to coincide with the line from which we count the volume-per-flux, i.e., with the  $y$ -axis:  $\Phi_e(0, y) \equiv 0$ .

With these definitions we now show that in steady state ideal incompressible electron MHD the two functions are just proportional to each other:

$$\Phi_e(x, y) = -cE_z V(x, y). \quad (26)$$

where  $E_z$  is the uniform electric field in the  $z$ -direction.

To prove this, let us consider the variation of  $\Phi_e$  *along the poloidal magnetic field* and show that it is proportional to that of  $V$ . Consider two points lying close to each other on the same poloidal field line  $\Psi$ , and let  $\Delta l_{\text{pol}}$  be the infinitesimal separation between these two points along the poloidal field. From equation (24), the difference between the volume-per-flux of these two points is

$$\Delta V = \frac{\Delta l_{\text{pol}}}{B_{\text{pol}}}. \quad (27)$$

On the other hand, the difference between the values of the electron stream function at these two points can be expressed in terms of the perpendicular component of the poloidal

electron velocity

$$\mathbf{v}_{\text{pol},\perp}^{(e)} = [\nabla\Phi_e \times \hat{z}]_{\perp} = \frac{\Delta\Phi_e}{\Delta l_{\text{pol}}} [\mathbf{b}_{\text{pol}} \times \hat{z}] = -\frac{\Delta\Phi_e}{\Delta l_{\text{pol}} B_{\text{pol}}} \nabla\Psi, \quad (28)$$

where  $\mathbf{b}_{\text{pol}}$  is the unit vector along the poloidal magnetic field. On the other hand,  $\mathbf{v}_{\text{pol},\perp}^{(e)}$  can be deduced from the generalized Ohm law. Neglecting resistive and inertial terms and taking into account that  $\partial_z p_e = 0$ , the toroidal component of this law can be written as

$$c E_z \hat{z} + [\mathbf{v}_{\text{pol},\perp}^{(e)} \times \mathbf{B}_{\text{pol}}] = 0. \quad (29)$$

By taking the vector product of this equation with  $\mathbf{B}_{\text{pol}}$ , we get

$$\mathbf{v}_{\text{pol},\perp}^{(e)} = c \frac{E_z \hat{z} \times \mathbf{B}_{\text{pol}}}{B_{\text{pol}}^2} = c \frac{E_z}{B_{\text{pol}}} [\hat{z} \times \mathbf{b}_{\text{pol}}] = c \frac{E_z}{B_{\text{pol}}^2} \nabla\Psi. \quad (30)$$

Comparing equations (28) and (30) we immediately see that

$$\Delta\Phi_e = -\frac{cE_z}{B_{\text{pol}}} \Delta l_{\text{pol}}, \quad (31)$$

which, together with equation (27), gives

$$\Delta\Phi_e = -cE_z \Delta V. \quad (32)$$

Because we choose to count the volume-per-flux from the  $\Phi_e = 0$  electron streamline, then, summing this equation along each field line, we get equation (26), as desired. But we can actually proceed more directly. Let us consider the variations of  $\Phi_e$  and  $V$  *across the poloidal field*. For this, consider a single poloidal field line  $\Psi$  at two neighboring moments of time,  $t_1$  and  $t_2 = t_1 + \Delta t$ . Consider a certain point  $A_1$  on the field line at  $t = t_1$  and see it  $\mathbf{E} \times \mathbf{B}$ -drift with the field line to a new location  $A_2$  at  $t = t_2$ . The corresponding change in the volume-per-flux is due to the plasma that has flowed in along the poloidal field past this point during the time  $\Delta t$ :

$$\Delta V \equiv V(A_2) - V(A_1) = -\frac{v_{\text{pol},\parallel} \Delta t}{B_{\text{pol}}}. \quad (33)$$



At the same time, this parallel inflow of the plasma results in a change in  $\Phi_e$  between points  $A_1$  and  $A_2$ :

$$\Delta\Phi_e \equiv \Phi_e(A_2) - \Phi_e(A_1) = v_{\text{pol},\parallel} (\Delta\mathbf{s}_{\text{pol},\perp} \cdot [\hat{z} \times \mathbf{b}_{\text{pol}}]), \quad (34)$$

where the poloidal displacement vector  $\Delta\mathbf{s}_{\text{pol},\perp}$  in the direction perpendicular to the poloidal magnetic field is given by the  $\mathbf{E} \times \mathbf{B}$  drift:

$$\Delta\mathbf{s}_{\text{pol},\perp} = \mathbf{v}_{\perp,\text{pol}}\Delta t = \Delta t \frac{cE_z}{B_{\text{pol}}} [\hat{z} \times \mathbf{b}_{\text{pol}}]. \quad (35)$$

Thus, we get

$$\Delta\Phi_e = v_{\text{pol},\parallel}\Delta t \frac{cE_z}{B_{\text{pol}}}, \quad (36)$$

and comparing this result with equation (33), we again see that

$$\Delta\Phi_e = -cE_z\Delta V. \quad (37)$$

A similar derivation also holds in the downstream region.

Thus we have shown that the variation of the electron stream function  $\Phi_e$  in both parallel and perpendicular directions is equal to  $-cE_z$  times the corresponding variation in the volume per flux integral  $V$ . Using the convention of counting both  $\Phi_e$  and  $V$  starting from the y-axis, we again arrive at the relationship (26).

The second important relationship is the proportionality between the electron stream function  $\Phi_e$  and the electron contribution to the toroidal field  $B_z$ . This well-known relationship follows immediately from Ampere's law and the reflection symmetry conditions [ $B_z(x=0, y) = 0 = \Phi_e(x=0, y)$  upstream and  $B_z(x, y=0) = 0 = \Phi_e(x, y=0)$  downstream]. It reads:

$$B_z(x, y) = -D\Phi_e(x, y), \quad (38)$$

with the coefficient  $D$  given by

$$D \equiv \frac{4\pi n_e e}{c} = \frac{\sqrt{4\pi\rho}}{d_i} = \frac{B_0}{d_i V_A}. \quad (39)$$

(Here  $B_0$  is an arbitrary normalization field used in the definition of  $V_A$ .)

Note that the coefficient  $D$  defined by equation (39) is constant for the case of uniform density considered here. If the density were not uniform, we would get a similar result  $B_z \sim \Phi_e$ , if the electron density is incorporated into  $\Phi_e$ , i.e., if  $\Phi_e$  is defined by  $n_e \mathbf{v}_{\text{pol}}^{(e)} = [\nabla \times (\Phi_e \hat{z})]$ . Similarly, equation (26) would be valid if  $V$  is understood as the number of electrons per unit flux, instead of the volume-per-flux.

Combining this equations (38) and (26) we immediately see that

$$B_z = cDE_z V. \quad (40)$$

This result is important because it shows how, in eMHD, one can immediately determine  $B_z$  once the poloidal field structure is known, without having to solve any partial differential equations! One just has to compute the volume-per-flux integral given by equation (24) upstream and the corresponding expression downstream, and the toroidal field will be just the constant  $cDE_z$  times it.

Already by itself, the simple relationship (38) is important, because it means that, neglecting ion currents, the toroidal field is constant along the poloidal electron streamlines; its value is simply transported in space by the poloidal electron flow:

$$(\mathbf{v}_{\text{pol}}^{(e)} \cdot \nabla) B_z = -DB_0 [\nabla \Phi_e \times \hat{z}] \cdot \nabla \Phi_e \equiv 0, \quad (41)$$

where  $\mathbf{v}_{\text{pol}}^{(e)}$  is the total poloidal electron velocity including the parallel flow.

This result suggests that the toroidal magnetic field cannot be created locally, in the inner part of the reconnection region (where ion current is unimportant); instead, it has to

be brought into this region by the convergent electron flow. The toroidal field thus has to be generated in the outer parts of the layer, where the ion-current contribution to  $B_z$  is not negligible. We discuss this generation process in Sec. III C.

In addition, as long as electrons are completely frozen into the magnetic field, the evolution equation for the toroidal magnetic field, i.e., the toroidal component of the magnetic induction equation, tells us that

$$v_{\text{pol}}^{(e)} \cdot \nabla B_z = B_{\text{pol}} \cdot \nabla v_z^{(e)}, \quad (42)$$

in a steady state. Therefore, since the left-hand side (LHS) of this equality is zero, as we have just shown, the right-hand side (RHS) is also zero. That is, the toroidal electron velocity and hence the toroidal current density  $j_z = -en_e v_z^{(e)}$  are uniform along poloidal field lines as long as one can neglect the ion current. Since from Ampere's law the toroidal current density is simply proportional to the Laplacian of  $\Psi$ , we see that in order to get a consistent solution, one cannot pick the poloidal flux function arbitrarily; one has to impose the condition that  $\nabla^2 \Psi = F(\Psi)$ . For example, the simple X-point poloidal field configuration considered in Sec. II C trivially satisfies this condition with  $F(\Psi) \equiv \text{const}$ .

The above observation also means that within the pure eMHD framework with no ion currents one cannot really apply the well-known conventional explanation, first introduced in Ref. [14], of how the quadrupole field is generated. By itself, this argument does not rely on neglecting ion currents. Instead it relies on the fact that magnetic field is completely frozen into the electron fluid. The toroidal field is then viewed as being produced from the poloidal magnetic field as a result of the differential stretching in the toroidal direction by the electron flow. This argument thus approaches the generation of the quadrupole field from a different angle: it presents the point of view of the ideal eMHD Ohm's law (with

the Hall term), instead of using Ampere's law. It basically goes like this: as a field line is advected into the reconnection layer, the electrons on it start to move toroidally (to carry some of the reconnection current) and they do it differentially, moving faster on the central piece of the field line. Since the magnetic field is frozen into the electron fluid, the field line bends out of the reconnection plane, resulting in the quadrupole pattern of the toroidal field. This line of thought is actually quantified by equation (41). That is, the toroidal field is created by the stretching due to the non-uniformity of  $v_z^{(e)}$  along a poloidal field line (RHS) and is advected with the poloidal electron flow (LHS). But, as we have just seen, as long as one neglects ion currents, this equation becomes simply  $0 = 0$ . Thus, in order to understand toroidal field generation, one first needs to take ion currents into account (see Sec. III C for more discussion).

## B. The Shape of Field Lines in the $xz$ Plane

A complimentary way to look at the problem of the toroidal field generation is to analyze the shape of a field line projected on the  $xz$  plane, and see how it changes as the field lines move deeper into the layer. Let this shape be represented by the function  $z(x, \Psi)$ , which is given by

$$\frac{dz}{dx}\Big|_{\Psi} = \frac{B_z}{B_x}. \quad (43)$$

By integrating this along a field line we obtain:

$$\Delta z(x, \Psi) = z(x, \Psi) - z(0, \Psi) = \int_0^x B_z(x, \Psi) \frac{dx}{B_x(x, \Psi)} \Big|_{\Psi=\text{const}}. \quad (44)$$

Using equations (40) and (24), we then have

$$\Delta z(x, \Psi) = cDE_z \frac{V^2(x, \Psi)}{2}. \quad (45)$$

Note that the volume per flux is conserved by the motion of the electron fluid; this means that the  $x$ -position of an electron fluid element that stays on some constant- $\Psi$  field line changes with time in such a way as to keep  $V(x, \Psi)$  constant. Thus, if one follows a specific fluid element on a given moving field line  $\Psi$ , one finds that the toroidal distance  $\Delta z(x, \Psi)$  between this element and the point where the field line intersects the  $x = 0$  plane does not change with time. On the other hand, as we showed in Sec. II B, the fluid element moves along the *poloidal* magnetic field towards the  $y$  axis, and so its  $x$ -coordinate decreases. Therefore, the shape of the field line, which can be characterized by the function  $x(\Delta z)$ , changes with time. Interestingly, this change is not due to the differential toroidal stretching, as it is usually assumed, but is simply due to the fact that the two mirror-symmetric parts of the line are squeezed together by the converging poloidal flow.

### C. The Role of Ion Currents in the Generation of the Quadrupole Field

As we saw in Sec. III A, when the current due to the ions is neglected, the toroidal field is conserved along the electron streamlines and hence cannot be locally generated in the inner part of the reconnection layer. This indicates that, in order to explain how and where the toroidal field is generated, one has to bring the ions back into the picture. Deep inside the reconnection region, at  $x \ll L$  and  $y \ll \delta \sim d_i$ , the poloidal ion currents are indeed negligible and the above picture applies. On the other hand, in the upstream region well outside of the reconnection layer (i.e., for  $y \gg \delta$ ), ideal one-fluid MHD works well. In this region the electrons do move poloidally towards the reconnection layer with the  $\mathbf{E} \times \mathbf{B}$  velocity and the associated electron current would generate the toroidal field; however, the ions also move happily in the same direction and with the same speed. As a result, the

ion-current contribution to the toroidal field exactly cancels that of the electrons. Thus, the net toroidal field is zero in this region. From this we see that, in order to understand where the quadrupole toroidal field comes from, one has to look at the outskirts of the reconnection layer, where the ions become partly decoupled from the electrons, so that  $0 < |j_y^{(i)}| < |j_y^{(e)}|$ .

We can discuss the toroidal field generation from a different point of view, in terms of the shape  $z(x, \Psi)$  of a given field line  $\Psi$  as it is carried into the current layer by the electron flow. Far upstream, this field line lies entirely in the reconnection  $(x, y)$  plane, but as it moves into the reconnection region, it gradually starts to bend out of this plane. The toroidal electron velocity can be non-uniform along the line only in this transition region of non-zero ion current. Correspondingly, toroidal field is produced inside this region; subsequently, deeper inside the reconnection layer, the toroidal electron velocity becomes uniform along the line and hence the toroidal elongation freezes. Any further lengthening of the field line in the toroidal direction can be directly attributed to the “injection” of new segments of the field line in the transition region.

#### D. Toroidal Electron Velocity

To illustrate this picture, let us consider an extremely simplified model where the transition region is a razor-thin line  $y = \delta$ . In this example, the electrons and ions move together above  $y = \delta$  and so  $B_z(x, y > \delta) \equiv 0$ . Below this sharp boundary, we shall regard the ions as poloidally motionless, so that  $j_{\text{pol}}^{(i)}(y < \delta) = 0$  and hence the pure eMHD picture developed in the preceding sections applies. In addition, in this and in the next section we shall, for simplicity, neglect the toroidal component of the diamagnetic electron flow that results from poloidal electron pressure gradient.

Now let us consider a given field line  $\Psi$ ; as we follow its motion through the layer, the magnetic flux  $\Psi'$  between the separatrix and the given field line changes linearly in time according to  $\Psi'(t) = \Psi + cE_z t$ . Denote the  $x$ -coordinate of the point where this field line intersects the boundary  $y = \delta$  by  $x_\delta[\Psi'(t)] = x_\delta(\Psi + cE_z t)$ . For example, in the simple X-point configuration considered in Sec. II C, we have  $\bar{x}_\delta = [1 - 2\bar{\Psi}'(t)]^{1/2}$ . Next, because there is no toroidal field above  $y = \delta$ , we can set  $z = 0$  everywhere along this boundary, i.e.,  $z[x_\delta(\Psi'), \Psi] = 0$ . Then, using equation (45), we can express the toroidal coordinate of any fluid element  $(X(t), \Psi)$  on a given line  $\Psi$  as

$$z[X(t), \Psi] = \Delta z[X(t), \Psi] - \Delta z[x_\delta(\Psi'), \Psi] = cDE_z \frac{V^2[X(t), \Psi] - V_\delta^2(\Psi')}{2}, \quad (46)$$

where

$$V_\delta(\Psi') \equiv V[x_\delta(\Psi'(t)), \Psi]. \quad (47)$$

In this section we are interested in the toroidal electron velocity, so let us see how  $z(X, \Psi)$  changes with time following an electron fluid element. To do this, differentiate equation (46) with respect to time. When doing this we have to take into account that in ideal incompressible electron MHD the motion  $X(t)$  of a given fluid element is constrained by the condition that  $V[X(t), \Psi]$  remains constant. Then we have

$$v_z^{(e)}[X(t), \Psi] = \frac{d}{dt} z[X(t), \Psi] = -cDE_z \frac{d}{dt} \left[ \frac{V_\delta^2(\Psi')}{2} \right] = -c^2 DE_z^2 \frac{d}{d\Psi'} \left[ \frac{V_\delta^2(\Psi')}{2} \right], \quad (48)$$

since  $d\Psi'/dt = cE_z$ . Thus, the velocity is proportional to the flux derivative of the square of a flux tube's entire volume up to the boundary  $y = \delta$ .

One sees that the toroidal velocity is constant along field lines but, in general, varies from line to line. In particular, the volume-per-flux  $V_\delta(\Psi')$  grows rapidly near the separatrix and so  $v_z^{(e)}$  becomes very large there. This appears to be inconsistent, for instance, with the simple

X-point configuration considered in Sec. II C; indeed, the particular form of the poloidal flux function in that example corresponded to a flat toroidal current profile,  $j_z = \text{const}$ , and hence  $v_z^{(e)} = \text{const}$ . The way to resolve this discrepancy is to note that the sharp rise in the toroidal current density that corresponds to equation (48), leads to only a relatively small change in the poloidal field structure. Moreover, this change is actually consistent with that expected from the back-reaction of the toroidal magnetic field pressure. This back-reaction arises because, as one approaches the separatrix, the toroidal field increases sharply and starts to play an important dynamical role. In particular, it modifies the poloidal field structure through the vertical pressure balance condition; the poloidal field decreases near the separatrix and this leads (by Ampere's law) to an additional electric current, strongly concentrated near the separatrix. We can estimate this additional electric current as follows.

Let us write the vertical pressure balance as

$$B_{\text{pol}}^2 + B_z^2 = B_0^2 - 8\pi P = B_0^2 \bar{y}^2, \quad (49)$$

where we have assumed that the total plasma pressure  $P$  has a parabolic profile:  $8\pi P = B_0^2(1 - \bar{y}^2)$ . If we neglect the toroidal field pressure term in this equation, we then recover our original poloidal field profile  $B_{\text{pol}} \approx B_x = B_0 \bar{y}$ , which corresponds to uniform toroidal current. Note, however, that even if  $B_x$  itself is small, its rate of change may become important near the separatrix, so that the corresponding small but rapid change in  $B_x$  results in a large contribution to the toroidal current. Indeed, differentiating equation (49) with respect to  $\bar{y}$ , we get

$$\frac{dB_{\text{pol}}^2}{d\bar{y}} = 2B_x \frac{dB_x}{d\bar{y}} \simeq -\frac{8\pi}{c} B_x \delta j_z = 2B_0^2 \bar{y} - \frac{dB_z^2}{d\bar{y}}. \quad (50)$$



Then, using equation (3) and (40), we find

$$j_z = -\frac{c}{4\pi} \left[ \frac{B_0}{\delta} - c^2 D^2 E_z^2 \frac{\partial}{\partial \Psi'} \left( \frac{V^2(x, \Psi')}{2} \right) \right] \simeq n_e e c^2 D E_z^2 \frac{\partial}{\partial \Psi'} \left[ \frac{V^2(x, \Psi')}{2} \right], \quad (51)$$

and so, assuming that the additional toroidal current is predominantly carried by electrons,

$$v_z^{(e)} \simeq -c^2 D E_z^2 \frac{\partial}{\partial \Psi'} \left[ \frac{V^2(x, \Psi')}{2} \right] \quad (52)$$

— an expression that is very similar, although not quite the same, as equation (48).

Finally, for reference, let us give expressions for  $V_\delta(\Psi')$  and  $v_z^{(e)}$  that correspond to the simple X-point configuration considered in Sec. II C. First, according to equation (10), we have

$$V_\delta(\bar{\Psi}') = \frac{L}{B_0} \log \left| \frac{1 + \sqrt{1 - 2\bar{\Psi}'}}{\sqrt{2\bar{\Psi}'}} \right| = \frac{L}{2B_0} \log \left| \frac{1 + \bar{x}_\delta(\Psi')}{1 - \bar{x}_\delta(\Psi')} \right|, \quad (53)$$

so that  $(d/d\bar{\Psi}') V_\delta(\bar{\Psi}') = -(L/2B_0) \bar{\Psi}' \bar{x}_\delta(\bar{\Psi}')$ .

Then, from equation (48) we obtain

$$v_z^{(e)}(\bar{\Psi}') = -B_0 \delta D |\bar{E}|^2 V_\delta(\bar{\Psi}') \frac{d}{d\bar{\Psi}'} V_\delta(\bar{\Psi}') = \frac{L^2 \delta D}{2B_0} \frac{|\bar{E}|^2}{2\bar{\Psi}' \bar{x}_\delta(\bar{\Psi}')} \log \left| \frac{1 + \bar{x}_\delta(\bar{\Psi}')}{1 - \bar{x}_\delta(\bar{\Psi}')} \right|. \quad (54)$$

Finally, using definition (21), we can write this as

$$v_z^{(e)}(\bar{\Psi}') = \frac{LQ|\bar{E}|}{4\bar{\Psi}' \bar{x}_\delta(\bar{\Psi}')} \log \left| \frac{1 + \bar{x}_\delta(\bar{\Psi}')}{1 - \bar{x}_\delta(\bar{\Psi}')} \right|. \quad (55)$$

### E. Finite Electron-Inertia Effects

We can use the above formula for  $v_z^{(e)}$  to estimate when the electron inertial term stops being negligible in the toroidal component of the electron equation of motion. From that moment on, the finite electron inertia will be large enough to balance part of the toroidal electric field, and thus, the electrons will no longer have a pure  $\mathbf{E} \times \mathbf{B}$  velocity and will no

longer follow the field lines exactly. The inertial term (for a single electron) can be written as

$$m_e(\mathbf{v} \cdot \nabla) v_z^{(e)} \approx m_e(\mathbf{v}_{\text{pol},\perp} \cdot \nabla) v_z^{(e)} = m_e(\mathbf{v}_{\text{pol},\perp} \cdot \nabla \Psi') \frac{dv_z^{(e)}}{d\Psi'}, \quad (56)$$

where we take into account that  $v_z^{(e)}$  is constant along field lines and so is a function of  $\Psi'$  only. Using expression (30) for  $\mathbf{v}_{\text{pol},\perp}$ , we get

$$m_e(\mathbf{v} \cdot \nabla) v_z^{(e)} \approx m_e c E_z \frac{dv_z^{(e)}}{d\Psi'}. \quad (57)$$

Then, using (48), we get

$$m_e(\mathbf{v} \cdot \nabla) v_z^{(e)} \approx -m_e c^3 E_z^3 D \frac{d^2}{d(\Psi')^2} \left[ \frac{V_\delta^2(\Psi')}{2} \right]. \quad (58)$$

We can no longer neglect electron inertia when this term becomes comparable to the toroidal electric force on an electron,  $-eE_z$ . We estimate this to happen for values of  $\Psi'$  of order of  $\Psi'_*$ , which is obtained as the solution of the equation

$$[V_\delta^2(\Psi')]'' = \frac{2e}{m_e c D} \frac{1}{c^2 E_z^2} = \frac{1}{2\pi n_e m_e} \frac{1}{c^2 E_z^2}. \quad (59)$$

We can apply this estimate to our simple X-point example, for which  $V_\delta(\Psi')$  is given by (53). Since we expect the electron inertia to become important only near the separatrix,  $\bar{\Psi}' \ll 1$ , we can approximately write  $V_\delta(\Psi') \simeq -(L/2B_0) \log \bar{\Psi}'$ , and then

$$v_z^{(e)} \approx -\frac{1}{2} QL|\bar{E}| \frac{\log \bar{\Psi}'}{2\bar{\Psi}'}. \quad (60)$$

The inertial term in the toroidal component of Ohm's law is then estimated, with the help of equation (57), as

$$m_e(\mathbf{v} \cdot \nabla) v_z^{(e)} \approx m_e \bar{E} \frac{dv_z^{(e)}}{d\Psi'} \approx -m_e QL|\bar{E}|^2 \frac{\log \bar{\Psi}'}{4\bar{\Psi}'^2}, \quad (61)$$

where we recall that  $\bar{E} < 0$  in our solution. After some manipulation we can write the condition on  $\bar{\Psi}'_*$  as

$$\frac{2\bar{\Psi}'_*}{\sqrt{|\log \bar{\Psi}'_*|}} = Q \frac{d_e}{\delta} = \sqrt{\frac{m_e}{m_i}} \frac{Lv_{\text{rec}}}{\delta V_A} = O\left[\left(\frac{m_e}{m_i}\right)^{1/2}\right], \quad (62)$$

where we use equation (22) and define  $d_e \equiv c/\omega_{pe}$ . Thus,

$$\bar{\Psi}'_* \sim \sqrt{\frac{m_e}{m_i} \log \frac{m_i}{m_e}}. \quad (63)$$

When traced to the  $y$  axis, this critical field line corresponds to a distance

$$y_* \sim \left(\frac{m_e}{m_i} \log \frac{m_i}{m_e}\right)^{1/4} \delta \quad (64)$$

from the X-point. (This is of order  $\delta/4$  for hydrogen plasma). It is essentially (apart from the logarithmic factor) of the same order as the distance at which electrons become demagnetized, i.e., comparable to the size of electron figure-eight and betatron orbits.

## F. The bipolar poloidal electric field

Why do field lines move in the toroidal direction as they enter the layer? To answer this question, we need to consider the toroidal projection of the perpendicular (to the total magnetic field) electron velocity,  $v_{\perp,z}$ . Let us locally introduce a rotated orthonormal coordinate system  $(x', y', z)$  where  $x'$  is the direction along the poloidal magnetic field and  $y'$  is the direction in the poloidal plane which is perpendicular to the poloidal magnetic field. Taking into account the electron pressure (which we assume isotropic) but neglecting the electron inertia, we can express  $v_{\perp,z}^{(e)}$  as

$$\begin{aligned} v_{\perp,z}^{(e)} &= c \frac{[\mathbf{E}_{\text{pol}} \times \mathbf{B}_{\text{pol}}]_z}{B^2} + c \frac{[\nabla_{\text{pol}}(p_e/n_e e) \times \mathbf{B}_{\text{pol}}]_z}{B^2} \\ &= -c \frac{E_{y'} B_{\text{pol}}}{B^2} - c \frac{\partial_{y'}(p_e/n_e e) B_{\text{pol}}}{B^2}. \end{aligned} \quad (65)$$

This is a sum of two drifts: the  $\mathbf{E} \times \mathbf{B}$ -drift due to the poloidal electric field  $E_{y'}$  and the diamagnetic drift due to the electron pressure gradient. In principle, as long as the electron pressure is isotropic, these two terms can be combined by noticing that in a steady state the poloidal electric field is electrostatic,  $\mathbf{E}_{\text{pol}} = -\nabla\phi_2(x, y)$ , and defining  $\tilde{\phi}_2 \equiv \phi_2 - p_e/n_e e$ . Then,

$$v_{\perp,z}^{(e)} = c \frac{(\partial_{y'} \tilde{\phi}_2) B_{\text{pol}}}{B^2}. \quad (66)$$

However, an important point is that the diamagnetic drift is actually irrelevant, as far as the motion of field lines is concerned. In the presence of the pressure gradient, the field line velocity in fact differs from the electron perpendicular velocity and is given by just the  $\mathbf{E} \times \mathbf{B}$  velocity. Its  $z$ -component is

$$v_{B,z} = -c \frac{E_{y'} B_{\text{pol}}}{B^2}. \quad (67)$$

Thus, the field lines move toroidally because of  $E_{y'}$  that has a bipolar structure (see Fig. 3). The above argument suggests that, instead of saying that electrons pull the field lines in the toroidal direction in two-fluid reconnection, it is, in a sense, better to say that it is the magnetic field lines that start moving toroidally and pull the electrons with them. The poloidal electric field can therefore be viewed, similarly to the quadrupole toroidal magnetic field, as an important signature of Hall reconnection. It has in fact been detected with with the *Polar spacecraft* in the magnetopause [23], with the *Cluster spacecraft* in reconnection regions in the Earth magnetotail [24, 25] and in the SSX experiment [27]; it has also been seen in numerical simulations [17, 20, 21]. It is this electric field that pulls ions into the reconnection layer; as they move across the layer, they pick up the electrostatic potential difference of the order of  $\delta E_{y'}$ . This potential difference is large enough to accelerate ions (in the  $y$ -direction) up to about Alfvén speed. As a result, the ion  $v_y$ -distribution at the center

of the reconnection layer is well represented by two counter-streaming beams, which agrees both with numerical particle simulations [17, 20] and with spacecraft measurements [24]. Effectively, this process can be interpreted as a strong ion heating, providing the pressure support for the layer. In addition, ion collisions (with particles or with waves) may quickly isotropize the ion distribution function, leading to a true ion heating. The quadrupole toroidal magnetic field also plays an important role in the poloidal ion motion; in particular, as the ions are accelerated into the layer, the Lorentz force due to this field bends ion trajectories in the  $x$ -direction and thus leads to the ejection of ions out of the reconnection region.

For reference, we give an expression for the bipolar electric field for our simple X-point configuration example. To derive this expression, we make use of the toroidal electron velocity  $v_z^{(e)}$ , computed in Sec. III D.

First, from the  $y'$ -component of the ideal eMHD Ohm's law, we can write (neglecting electron pressure)

$$cE_{y'} = -v_z^{(e)}B_{x'} + v_{x'}^{(e)}B_z = -v_z^{(e)}B_{\text{pol}} + v_{\text{pol},\parallel}B_z = -B_{\text{pol}}(v_z^{(e)} - \lambda B_z), \quad (68)$$

where we express  $v_{x'} \equiv v_{\text{pol},\parallel}$  as  $\lambda B_{\text{pol}}$  as it is done in Appendix A. In the case of the simple X-point configuration of Sec. II C, we have at our disposal explicit expressions for all the ingredients that enter the above equation. Thus,  $B_{\text{pol}}$  is approximately equal to  $B_x$  given by equation (3);  $v_z^{(e)}$  is given by equation (55),  $\lambda$  by (A10), and  $B_z$  by (20). Putting it all together, we obtain

$$E_{y'}(\bar{x}, \bar{y}) = -\frac{Q}{2}|E_z|\frac{L}{\delta}\frac{1}{2\bar{\Psi}'}\left(\frac{\bar{y}}{\bar{x}_\delta(\bar{\Psi}')}\log\left|\frac{1+\bar{x}_\delta(\bar{\Psi}')}{1-\bar{x}_\delta(\bar{\Psi}')}\right| - \bar{x}\log\left|\frac{\bar{y}+\bar{x}}{\bar{y}-\bar{x}}\right|\right). \quad (69)$$

We see that, because of the  $L/\delta$  factor, this poloidal field can be considerably larger than the toroidal electric field.

## IV. CONCLUSIONS

In this paper we have investigated the structure of a reconnection layer in the Hall-MHD regime, in which electrons are well-magnetized inside the layer, whereas ions are not. Specifically, we have addressed the issue of how the quadrupole pattern of an out-of-plane (toroidal) magnetic field is generated inside a Hall-MHD reconnection region. This quadrupole pattern is commonly seen as an important feature of two-fluid physics that is at work in the reconnection process whenever the resistivity is small. It has been routinely observed both in numerical simulations and in space, and has recently been confirmed in a dedicated laboratory experiment [26]. In our view, this quadrupole pattern arises most naturally via the following mechanism.

Let us follow a flux tube as it enters the reconnection layer from the upstream region. As it moves deeper into the layer, the in-the-plane (poloidal) field in the central part of the tube weakens and so its cross-sectional area expands. This does not affect the ions very much. Let us assume that their density is constant throughout the inner part of the reconnection layer. Then, owing to charge neutrality, the electron density also has to be constant. Therefore, since the central part of the flux tube is expanding, electrons have to flow in into the layer along the poloidal magnetic field. Similarly, in the region downstream of the X-point, the flux tube is leaving the layer and so its cross-sectional area contracts. The electrons then are forced to flow along the poloidal field out of the layer. We thus obtain a circulating pattern of the electron current. In turn, it gives rise, through Ampere's law, to a toroidal magnetic field that automatically has a quadrupole structure. A more detailed qualitative description of this process is presented in Sec. II B.

We find that the most elegant and effective way to quantitatively analyze the behavior

of the system is in terms of the volume-per-flux integral  $V(x, \Psi)$ , which has a nice property that it is determined entirely by the poloidal magnetic field structure,  $\Psi(x, y)$ . We show that both the electron stream function  $\Phi_e$  and the toroidal magnetic field  $B_z$  are just proportional to  $V$ . Thus, once the poloidal field structure is specified, the poloidal electron velocity and all three components of the magnetic field are easily determined just by computing one integral, i.e., without solving any partial differential equations. In particular, we find that, as long as poloidal ion currents are neglected, the toroidal magnetic field is constant along electron streamlines. This means that, within a pure eMHD framework, the toroidal field cannot be produced! Instead, it has to come from the outer regions of the reconnection layer, where ion currents are not negligible.

We also find that the toroidal magnetic field is highly concentrated near the magnetic separatrix. We obtain explicit expressions for a simple X-point configuration and show that  $B_z$  has a logarithmic singularity at the separatrix. In reality, of course, the vertical pressure balance condition would prevent the toroidal field from being larger than the outside poloidal magnetic field  $B_0$ . This means that the pressure associated with the toroidal magnetic field becomes dynamically important near the separatrix and hence the poloidal field structure must be such as to keep the toroidal field finite. In addition, the singularity at the separatrix is removed by electron inertia. In order to estimate the electron inertial term in the toroidal component of the generalized Ohm law, however, one needs to know the toroidal electron velocity. To determine it, we consider how the full three-dimensional shape of a field line changes with time as the field line is advected into the layer. From this we deduce the toroidal electron velocity and hence estimate how rapidly the electron inertial term grows near the separatrix. This enables us to estimate size of the region around the separatrix where the electron inertia is not negligible.

It should be remarked that, in spite of the fact that our calculation diverges near the separatrix, it is perfectly valid in the upstream and downstream regions away from the separatrix. In fact, all our integrations are carried out from the  $x$  and  $y$  axes towards the separatrix and do not cross it.

Finally, we consider the well-known explanation of how the quadrupole toroidal field is produced (see, e.g., Ref. [14]). This explanation invokes the differential stretching of poloidal field lines by a non-uniform electron flow in the toroidal direction. So a natural question to ask is: what makes the electrons move in the toroidal direction inside the layer? We argue that the toroidal electron velocity is in fact the sum of the  $\mathbf{E} \times \mathbf{B}$  drift, associated with the bipolar poloidal electric field that points into the layer, and the diamagnetic drift due to electron pressure gradient. However, the latter does not lead to any motion of the field lines, and so the entire field-line stretching has to be attributed solely to the bipolar poloidal electric field. This illustrates the usefulness of this bipolar electric field as an important marker for two-fluid effects in the reconnection process. We also note that this electric field plays an important role in ion dynamics inside the reconnection layer. Namely, it is this field that is responsible for accelerating ions towards the midplane, leading to two counter-streaming ion beams and thus to an effective ion heating. The quadrupole toroidal magnetic field also plays an important role in ion dynamics as it diverts the two beams out of the layer (via the Lorentz force), thereby creating the expected stagnation-point pattern for the ion flow.



## Acknowledgments

We would like to thank M. Yamada, H. Ji, Y. Ren, A. Bhattacharjee, J. Drake, and M. Shay for stimulating and encouraging discussions. We are also very grateful to F. Mozer and to the anonymous referee for a number of very useful comments and suggestions that have improved the paper.

This research has been supported by the National Science Foundation Grant No. PHY-0215581 (PFC: Center for Magnetic Self-Organization in Laboratory and Astrophysical Plasmas).

## APPENDIX A: ALTERNATIVE DERIVATION OF THE ELECTRON VELOCITY FIELD IN THE SIMPLE X-POINT GEOMETRY

In this appendix we present an alternative derivation of the poloidal electron velocity (and hence the toroidal magnetic field) for our simple X-point magnetic structure described by equations (2) and (6). We make the same two basic assumptions: frozen-in law for the poloidal electron flow (which is not altered by the electron pressure) and incompressibility. Let us split the *poloidal* electron velocity field into two parts: parallel and perpendicular with respect to the *poloidal* magnetic field. According to equation (30), the perpendicular velocity is given by

$$\mathbf{v}_{\text{pol},\perp} = c \frac{E_z \hat{\mathbf{z}} \times \mathbf{B}_{\text{pol}}}{B_{\text{pol}}^2}. \quad (\text{A1})$$

In terms of the scaled variables introduced in Sec. II C, we can write the  $x$  and  $y$  components of this velocity as

$$\bar{v}_{\perp,x} = \frac{v_{\perp,x}}{L} = |\bar{E}| \left(\frac{\delta}{L}\right)^2 \frac{\bar{x}}{\bar{B}_{\text{pol}}^2}, \quad (\text{A2})$$

$$\bar{v}_{\perp,y} = \frac{v_{\perp,y}}{\delta} = -|\bar{E}| \frac{\bar{y}}{\bar{B}_{\text{pol}}^2} \simeq -|\bar{E}| \frac{1}{\bar{y}}. \quad (\text{A3})$$

The parallel part of the poloidal velocity can be written as

$$\mathbf{v}_{\text{pol},\parallel} = \lambda(\bar{x}, \bar{y}) \bar{\mathbf{B}}_{\text{pol}}. \quad (\text{A4})$$

The total poloidal velocity field has to satisfy the incompressibility constraint,

$$\nabla \cdot \mathbf{v} = \nabla \cdot \mathbf{v}_{\text{pol},\perp} + \nabla \cdot \mathbf{v}_{\text{pol},\parallel} = 0. \quad (\text{A5})$$

Using expressions (A2)—(A3), we can write the divergence of the perpendicular poloidal velocity, to lowest order in  $\delta/L$ , as

$$\nabla \cdot \mathbf{v}_{\text{pol},\perp} = \bar{\nabla} \cdot \bar{\mathbf{v}}_{\text{pol},\perp} \simeq \partial_{\bar{y}} \bar{v}_{\perp,y} = \frac{|\bar{E}|}{\bar{y}^2}. \quad (\text{A6})$$

The divergence of the parallel velocity can be written as

$$\nabla \cdot \mathbf{v}_{\text{pol},\parallel} = \nabla \cdot (\lambda \mathbf{B}_{\text{pol}}) = \mathbf{B}_{\text{pol}} \cdot \nabla \lambda = B_{\text{pol}} \partial_{l_{\parallel}} \lambda, \quad (\text{A7})$$

where  $l_{\parallel}$  is the path length along a poloidal field line. Since the divergence of the total velocity must be zero, we get an expression for  $\lambda$ :

$$\lambda(\bar{\Psi}, \bar{x}) = - \int_0^{l_{\parallel}(\bar{x})} (\nabla \cdot \mathbf{v}_{\text{pol},\perp}) \frac{dl_{\parallel}}{B_{\text{pol}}} \Big|_{\bar{\Psi}} = - \frac{L}{B_0} \int_0^{\bar{x}} (\nabla \cdot \mathbf{v}_{\text{pol},\perp}) \frac{d\bar{x}}{\bar{B}_x} \Big|_{\bar{\Psi}}. \quad (\text{A8})$$

Using our expression (A6) for  $\nabla \cdot \mathbf{v}_{\text{pol},\perp}$ , we get

$$\lambda(\bar{\Psi}, \bar{x}) = - \frac{L}{B_0} |\bar{E}| \int_0^{\bar{x}} \frac{d\bar{x}}{\bar{y}^3(\bar{x}, \bar{\Psi})} \Big|_{\bar{\Psi}}. \quad (\text{A9})$$

Using equation (7) for the field line shape,  $\bar{y}(\bar{x}, \bar{\Psi})$ , we have

$$\lambda(\bar{\Psi}, \bar{x}) = - \frac{L}{B_0} |\bar{E}| \int_0^{\bar{x}} \frac{d\bar{x}}{(2\bar{\Psi} + \bar{x}^2)^{3/2}} \Big|_{\bar{\Psi}} = - \frac{L}{B_0} \frac{|\bar{E}|}{2\bar{\Psi}} \frac{\bar{x}}{\bar{y}}. \quad (\text{A10})$$

Correspondingly, the components of the parallel velocity are

$$\bar{v}_{\parallel,x} = \frac{v_{\parallel,x}}{L} = \frac{\lambda}{L} B_x = -\frac{|\bar{E}|}{2\bar{\Psi}} \bar{x}, \quad (\text{A11})$$

$$\bar{v}_{\parallel,y} = \frac{v_{\parallel,y}}{\delta} = \frac{\lambda}{\delta} B_y = -\frac{|\bar{E}|}{2\bar{\Psi}} \frac{\bar{x}^2}{\bar{y}}. \quad (\text{A12})$$

By combining this result with the components of the perpendicular velocity, we finally get

$$\bar{v}_x = \bar{v}_{\parallel,x} + \bar{v}_{\perp,x} \simeq \bar{v}_{\parallel,x} = -\frac{|\bar{E}|}{2\bar{\Psi}} \bar{x}, \quad (\text{A13})$$

$$\bar{v}_y = \bar{v}_{\parallel,y} + \bar{v}_{\perp,y} = -\frac{|\bar{E}|}{\bar{y}} \left( \frac{\bar{x}^2}{2\bar{\Psi}} + 1 \right) = -\frac{|\bar{E}|}{2\bar{\Psi}} \bar{y}, \quad (\text{A14})$$

— in complete agreement with our calculation in Sec. II C!

## APPENDIX B: 2D STATIONARY IDEAL ELECTRON MHD: GENERAL FORMALISM

In this section we describe a general formalism for analyzing a translationally-symmetric electron-MHD system in a steady state. We assume here that the electron density is uniform. In addition, we neglect any ion currents, both toroidal and poloidal; this assumption is valid if, for example, the ion temperature is negligible. We also neglect electron inertia; however, we do include an isotropic electron pressure in our equations.

In full generality, the system is described by three vector fields:  $\mathbf{B}$ ,  $\mathbf{v}^{(e)}$ , and  $\mathbf{E}$ , and a scalar electron pressure  $p_e$ ; it is thus quite complicated. However, these fields are not all independent of each other. It turns out that the eMHD framework is so constraining that, with the help from the time-stationarity and translational symmetry conditions, the magnetic and electron velocity fields can be expressed in terms of only a single one-dimensional function and a constant. In the following, we outline how this is done.

First, from  $\nabla \cdot \mathbf{B} = 0$  and the translational symmetry with respect to  $z$ , the magnetic field can be represented by two functions: the poloidal flux function  $\Psi(x, y)$  (which in this section is measured from the X-point  $x = 0 = y$ ) and the toroidal field  $B_z(x, y)$ :

$$\mathbf{B} = B_z \hat{z} + \mathbf{B}_{\text{pol}} = B_z \hat{z} + \nabla \times [\Psi \hat{z}] = B_z \hat{z} + [\nabla \Psi \times \hat{z}]. \quad (\text{B1})$$

The poloidal magnetic field components are

$$B_x = \partial_y \Psi; \quad (\text{B2})$$

$$B_y = -\partial_x \Psi. \quad (\text{B3})$$

Next, the electron velocity  $\mathbf{v}^{(e)}$  is completely determined in terms of the magnetic field by Ampere's law:

$$\mathbf{v}^{(e)} = -\frac{j_e}{n_e e} = -\frac{1}{D} \nabla \times \mathbf{B}, \quad (\text{B4})$$

where  $D \equiv 4\pi n_e e/c$ . In particular,

$$v_z^{(e)} = -\frac{1}{D} [\nabla \times [\nabla \times (\Psi \hat{z})]]_z = \frac{1}{D} \nabla^2 \Psi, \quad (\text{B5})$$

$$\mathbf{v}_{\text{pol}}^{(e)} = -\frac{1}{D} [\nabla \times (B_z \hat{z})] = -\frac{1}{D} [\nabla B_z \times \hat{z}]. \quad (\text{B6})$$

Since the density is uniform,  $D$  is constant.

Now let us turn to the electric field  $\mathbf{E}$ . Generally speaking, the overall global magnetic configuration evolves as a result of reconnection. In particular, there is a continuous transfer of poloidal magnetic flux through the X-point and hence there is a non-zero toroidal electric field at that point. This electric field is a measure of the reconnection rate; it is inductive in nature. However, if the reconnection process is changing quasi-statically on the dynamical (Alfvén) time scale, then locally, inside and around the layer, the magnetic field is essentially stationary,  $\partial_t \mathbf{B} = 0$ . Faraday's law then gives  $\nabla \times \mathbf{E} = 0$ . Because of the translational

symmetry the toroidal electric field then has to be uniform; then, the poloidal electric field has to be potential:

$$E_z(x, y) = \text{const}; \quad (\text{B7})$$

$$\mathbf{E}_{\text{pol}}(x, y) = -\nabla\phi_2(x, y). \quad (\text{B8})$$

Thus, the full three-dimensional electric field is described by a constant inductive reconnection field  $E_z$  and a 2D electrostatic potential  $\phi_2(x, y)$ .

This electric field is tied to the magnetic and velocity fields by the generalized Ohm law, i.e., the electron equation of motion. Neglecting the inertial and resistive terms but taking into account the Hall term and the electron pressure gradient term, this law becomes

$$\mathbf{E} + \frac{1}{c} [\mathbf{v}^{(e)} \times \mathbf{B}] + \frac{\nabla p_e}{n_e e} = 0. \quad (\text{B9})$$

By taking the vector product of this equation with  $\mathbf{B}$ , we get an expression for the perpendicular electron velocity:

$$\mathbf{v}_{\perp}^{(e)} = c \frac{\mathbf{E} \times \mathbf{B}}{B^2} + \frac{c}{n_e e} \frac{\nabla p_e \times \mathbf{B}}{B^2}. \quad (\text{B10})$$

The first term in this equation is the  $\mathbf{E} \times \mathbf{B}$  drift and the second term is the diamagnetic drift. Thus, the main effect of the pressure gradient term is the diamagnetic current. This current is in addition to that associated with the guiding center motion due to the  $\mathbf{E} \times \mathbf{B}$  drift and needs to be included in the total current that one substitutes in Ampere's law.

Provided that the electron density is uniform and the electron pressure tensor is isotropic, the diamagnetic currents do not lead to any substantial change in the mathematical structure of our formalism and are easily incorporated into our analysis. Indeed, combine the electric and pressure terms in Ohm's law into one by defining the modified electric field vector:

$$\tilde{\mathbf{E}} \equiv \mathbf{E} + \frac{1}{n_e e} \nabla p_e. \quad (\text{B11})$$

As we mentioned earlier, the poloidal electric field is potential,  $\mathbf{E}_{\text{pol}} = -\nabla\phi_2$ . Then, since we also assume that the electron density is uniform in space,  $\tilde{\mathbf{E}}_{\text{pol}}$  is also potential, i.e.,

$$\tilde{\mathbf{E}} = E_z \hat{z} - \nabla \tilde{\phi}_2 \equiv E_z \hat{z} - \nabla \left( \phi_2 - \frac{p_e}{n_e e} \right), \quad (\text{B12})$$

and so  $\mathbf{v}_{\perp}^{(e)} = c [\tilde{\mathbf{E}} \times \mathbf{B}] / B^2$ .

This means that we can take into account the diamagnetic currents resulting from the electron pressure gradient simply by working with  $\tilde{\phi}_2$  and  $\tilde{\mathbf{E}}$  instead of  $\phi_2$  and  $\mathbf{E}$ . Note that one thus cannot really distinguish between the electrostatic potential and the electron pressure, and hence between the  $\mathbf{E} \times \mathbf{B}$  drift and the diamagnetic drift, within the eMHD framework. This degeneracy however is not important; in particular, the magnetic and velocity fields can still be uniquely determined.

The generalized Ohm law can now be written as

$$\tilde{\mathbf{E}} = -\frac{1}{c} [\mathbf{v}^{(e)} \times \mathbf{B}]. \quad (\text{B13})$$

Using equations (B5)–(B6) for  $\mathbf{v}^{(e)}$  and equation (B1) for  $\mathbf{B}$ , we can then express the components of  $\tilde{\mathbf{E}}$  as

$$\tilde{E}_z = E_z = \frac{1}{cD} [\nabla B_z \times \nabla \Psi]_z = \text{const}, \quad (\text{B14})$$

$$\tilde{\mathbf{E}}_{\text{pol}} = -\frac{1}{cD} (\nabla^2 \Psi \nabla \Psi + B_z \nabla B_z). \quad (\text{B15})$$

But expressing  $\tilde{\mathbf{E}}_{\text{pol}}$  in terms of the 2D potential  $\tilde{\phi}_2(x, y)$  by equation (B12), we see that  $(\nabla^2 \Psi) \nabla \Psi = \nabla g(x, y)$ , where  $g \equiv cD \tilde{\phi}_2 - B_z^2/2$ . By taking the curl of this equation, we obtain  $\nabla \times (\nabla^2 \Psi \nabla \Psi) = \nabla(\nabla^2 \Psi) \times \nabla \Psi = 0$ , and hence  $\mathbf{B}_{\text{pol}} \cdot \nabla(\nabla^2 \Psi) = 0$ . That is, the toroidal current,  $j_z \sim \nabla^2 \Psi$ , has to be constant along the field lines, and so must be a function of  $\Psi$  only:

$$\nabla^2 \Psi = F(\Psi). \quad (\text{B16})$$

This equation is a necessary condition for the system to have a stationary solution, provided that the ion currents are neglected. This result is consistent with our earlier (Sec. III A) finding based on the analysis of the toroidal component of the eMHD magnetic induction equation,  $\mathbf{B}_{\text{pol}} \cdot \nabla v_z = \mathbf{v}_{\text{pol}} \cdot \nabla B_z$ . Notice that, in the main part of the paper we considered a general poloidal field configuration which could be supported by both ion and electron toroidal currents and thus equation (B16) did not need to be satisfied. However, the poloidal field structure of our specific example of Sec. II C does satisfy this equation, which means that it could be produced purely by electron toroidal currents with no ion contribution.

Once condition (B16) is satisfied, we can use the above formalism to compute, one by one, all the other electro-magnetic quantities. To do this for a given function  $F(\Psi)$ , one first solves the Poisson equation (B16) to find  $\Psi(x, y)$ , and then computes the poloidal magnetic field  $\mathbf{B}_{\text{pol}}$  and the toroidal velocity  $v_z$  using equations (B1) and (B5). Next, one uses equation (B14), supplemented in the upstream region by the boundary condition  $B_z(x = 0, y) = 0$  [and by  $B_z(x, y = 0) = 0$  in the downstream region], to calculate the toroidal magnetic field  $B_z$ . Indeed, the meaning of this equation is that the rate of change of the toroidal field along a poloidal field line is equal to  $cDE_z/B_{\text{pol}}$ :

$$\mathbf{B}_{\text{pol}} \cdot \nabla B_z = [\nabla \Psi \times \hat{z}] \cdot \nabla B_z = [\nabla B_z \times \nabla \Psi] \cdot \hat{z} = cDE_z = \text{const}. \quad (\text{B17})$$

Therefore, using the symmetry boundary condition at the  $y$ -axis, the toroidal field can be immediately obtained by integration along the field line:

$$B_z(x, \Psi) = cDE_z V(x, \Psi) \equiv cDE_z \int_0^x \frac{dl_{\text{pol}}}{B_{\text{pol}}(l_{\text{pol}}, \Psi)} = cDE_z \int_0^x \frac{dx'}{B_x(x', \Psi)}. \quad (\text{B18})$$

Finally, one uses equation (B6) to determine the poloidal electron velocity and equation (B15) to determine the modified poloidal electric field.

This concludes the solution of the problem for a given poloidal field. The question of what determines the poloidal magnetic field structure lies beyond the scope of this paper. Here we just would like to remark that this structure is going to be affected by the pressure associated with the toroidal magnetic field. Specifically, since the toroidal field is strongest near the separatrix, it will push the flux surfaces apart, resulting in a weaker poloidal field near the separatrix. This effect has to be taken into account self-consistently.

---

- [1] M. Yamada, H. Ji, S. Hsu, T. Carter, R. Kulsrud, N. Bertz, F. Jobes, Y. Ono, and F. Perkins, *Phys. Plasmas*, **4**, 1936 (1997).
- [2] P. A. Sweet, in *Electromagnetic Phenomena in Cosmical Physics*, ed. B. Lehnert, (Cambridge University Press, New York, 1958), p. 123.
- [3] E. N. Parker, *J. Geophys. Res.*, **62**, 509 (1957).
- [4] E. N. Parker, *ApJ Supplement*, **8**, 177 (1963).
- [5] H. E. Petschek, in *AAS-NASA Symposium on Solar Flares*, (National Aeronautics and Space Administration, Washington, DC, 1964), NASA SP50, 425.
- [6] D. Biskamp, *Phys. Fluids* **29**, 1520 (1986).
- [7] M. Scholer, *J. Geophys. Res.*, **94**, 8805 (1989)
- [8] D. A. Uzdensky and R. M. Kulsrud, *Phys. Plasmas*, **7**, 4018 (2000).
- [9] R. M. Kulsrud, *Earth, Planets and Space*, **53**, 417 (2001).
- [10] L. M. Mal'ushkin, T. Linde, and R. M. Kulsrud, *Phys. Plasmas*, **12**, 102902 (2005).
- [11] M. Ugai and T. Tsuda, *J. Plasma Phys.*, **17**, 337 (1977).
- [12] D. Biskamp and E. Schwarz, *Phys. Plasmas*, **8**, 4729 (2001).



- [13] B. U. Ö. Sonnerup, Magnetic Field Reconnection, in *Solar System Plasma Physics*, vol. 3, ed. L. T. Lanzerotti, C. F. Kennel, and E. N. Parker, (North-Holland, New York, 1979) p. 45.
- [14] M. E. Mandt, R. E. Denton, and J. F. Drake, *Geophys. Res. Lett.*, **21**, 73 (1994).
- [15] D. Biskamp, E. Schwarz, and J. F. Drake, *Phys. Plasmas*, **4**, 1002 (1997).
- [16] M. A. Shay and J. F. Drake, *Geophys. Res. Lett.*, **25**, 3759 (1998).
- [17] M. A. Shay, J. F. Drake, R. E. Denton, and D. Biskamp, *J. Geophys. Res.*, **103**, 9165 (1998).
- [18] T. Terasawa, *Geophys. Res. Lett.*, **10**, 475 (1983).
- [19] X. Wang, A. Bhattacharjee, and Z. W. Ma, *J. Geophys. Res.*, **105**, 27633 (2000).
- [20] K. Arzner and M. Scholer, *J. Geophys. Res.*, **106**, p. 3827 (2001).
- [21] P. L. Pritchett, *J. Geophys. Res.*, **106**, p. 25961 (2001).
- [22] J. A. Breslau and S. C. Jardin, *Phys. Plasmas*, **10**, 1291 (2003).
- [23] F. S. Mozer, S. D. Bale, and T. D. Phan, *Phys. Rev. Lett.*, **89**, 015002 (2002).
- [24] J. R. Wygant, C. A. Cattell, R. Lysak, Y. Song, J. Dombeck, J. McFadden, F. S. Mozer, C. W. Carlson, G. Parks, E. A. Lucek, A. Balogh, M. Andre, H. Reme, M. Hesse, and C. Mouikis, *J. Geophys. Res.*, **110**, A09206 (2005).
- [25] A. L. Borg, M. Oieroset, T. D. Phan, F. S. Mozer, A. Pedersen, C. Mouikis, J. P. McFadden, C. Twitty, A. Balogh, and H. Reme, *Geophys. Res. Lett.*, **32**, L19105 (2005).
- [26] Y. Ren, M. Yamada, S. Gerhardt, H. Ji, R. Kulsrud, and A. Kuritsin, *Phys. Rev. Lett.*, **95**, 055003 (2005).
- [27] W. H. Matthaeus, C. D. Cothran, M. Landerman, and M. R. Brown, *Geophys. Res. Lett.*, **32**, L23104 (2005).
- [28] Here, the term “2.5-D” refers, as usual, to a situation in which vectors are three-dimensional but all physical quantities are translationally invariant in one direction.

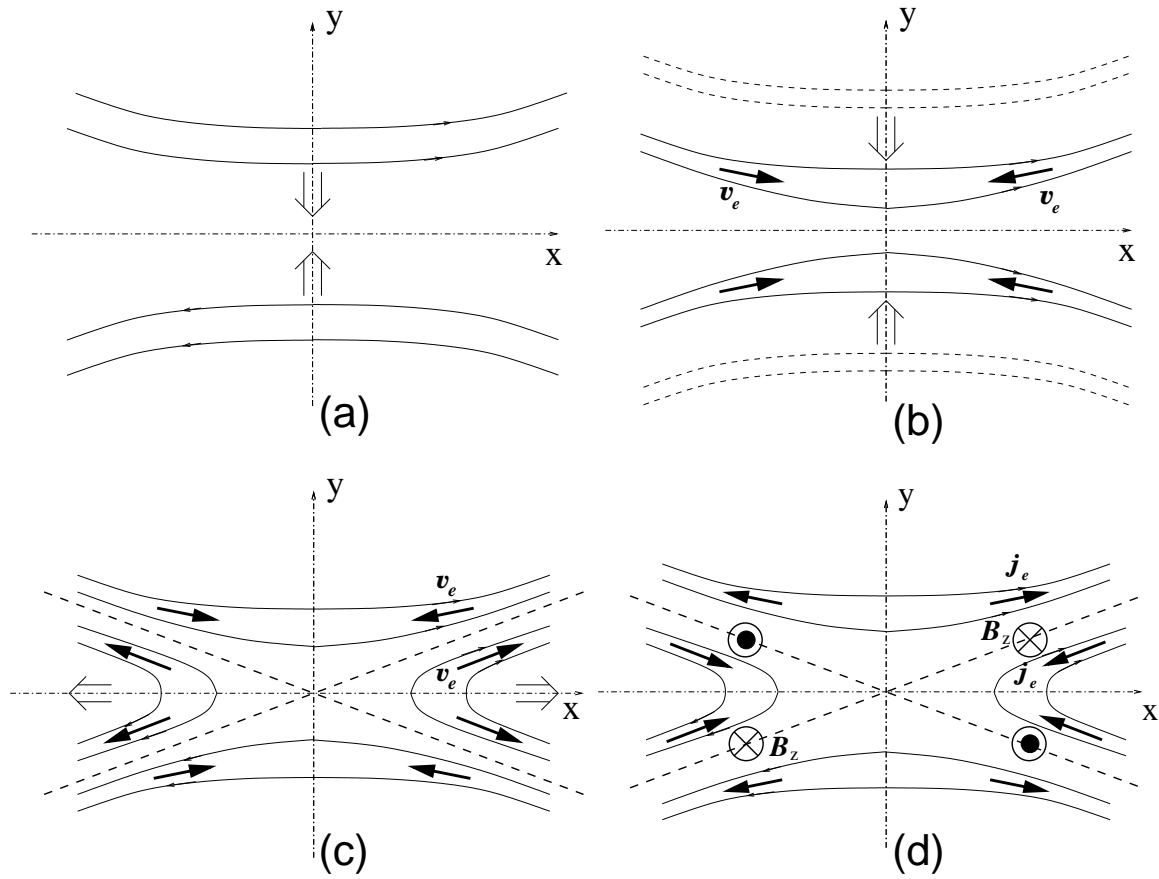


FIG. 1: The basic idea of out-of-plane field generation.

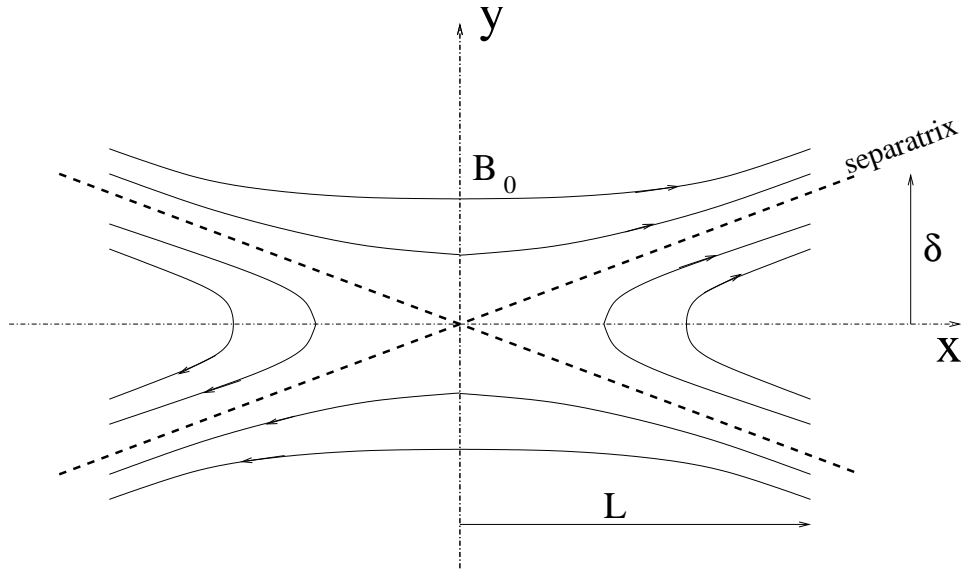


FIG. 2: Simple X-point configuration.

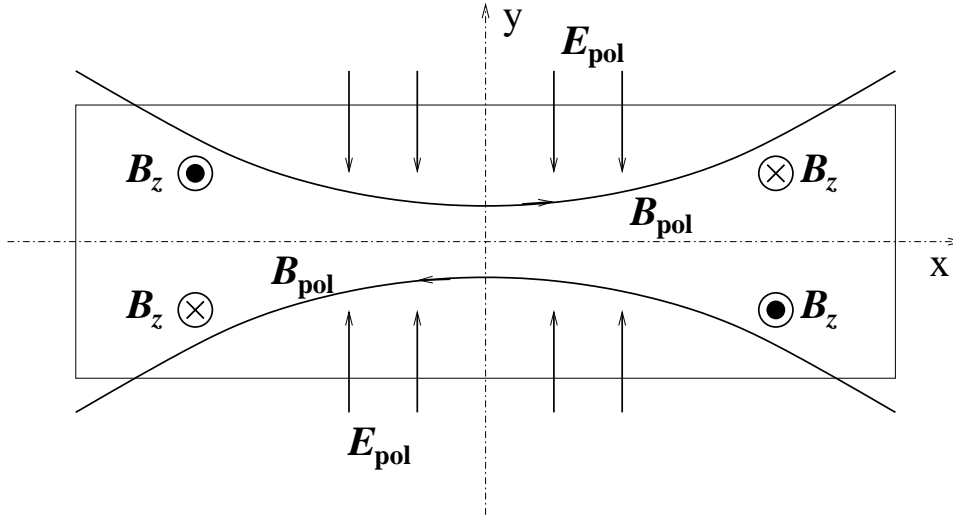


FIG. 3: Bipolar poloidal electric field.